

We thank the reviewers and editor for their comments, which have greatly improved this revised version. Below, we spell out how we have amended the manuscript to each specific comment. The 'tracked changes' version of the manuscript follows this.

### **Authors' response to the editorial comment:**

The comment by Astrid Kerkweg drew attention to an editorial requirement:

*"In particular, please note that for your paper, the following requirement has not been met in the Discussions paper:*

- *"The main paper must give the model name and version number (or other unique identifier) in the title."*

*Please add the names/acronyms (WASP/LGRTC) of the models used/developed and their version numbers to the title upon your revised submission to GMD. Yours,*

*Astrid Kerkweg"*

Thank you for drawing this editorial requirement to our attention. We have now included the model version described in the paper (WASP-LGRTC-1.0) within the new title:

*"A computationally efficient method for probabilistic local warming projections constrained by history matching and pattern scaling, demonstrated by WASP-LGRTC-1.0"*

### **Authors' responses to reviewer 1's comments:**

We thank reviewer 1, Dr. Christopher Smith, for important and insightful comments about our manuscript. Below we explain how we will use these comments to further improve our manuscript.

#### *"General comments*

*This paper describes a simple methodology for translating global mean surface temperature diagnostic output from a simple climate model (WASP, but in theory any model like MAGICC, FAIR, Hector could theoretically be used) into regional surface temperature changes using a pattern scaling approach. While this is not a necessarily new concept (see fldgen: <https://www.geosci-model-dev.net/12/1477/2019/>), it is appreciated that a quick and simple tool would be greatly useful for translating the output of simple climate models (e.g. from IAMs) to regional impacts. Additionally, there is a nice link from carbon emissions/carbon budgets to future carbon emissions. With this knowledge it could be possible to assess regional impacts as a function of the remaining carbon budget (e.g. to 1.5C)."*

**Point 1: Applicability of the spatial tool to any model capable of projecting global mean warming.** We agree that any model capable of generating probabilistic projections for global mean surface temperature could be combined with the spatial tools presented in this manuscript. This would then generate projections for the mean and standard deviation for future local warming. In our revised manuscript we highlight how the spatial tool can be coupled to any model projecting global mean warming, and not just the WASP model. This is first explicitly stated in the revised title of the manuscript, referring to a 'method' as opposed to a 'model': "A computationally efficient method for probabilistic local warming projections constrained by history matching and pattern scaling, demonstrated by WASP-LGRTC-1.0". We then explicitly state that we are presenting a method that can be coupled to any efficient model in the manuscript, e.g. page 1, Lines 17-20:

“This study presents a computationally efficient method for generating probabilistic projections of local warming across the globe, using a pattern scaling approach derived from the Climate Model Intercomparison Project phase 5 (CMIP5) ensemble, that can be coupled to any efficient model ensemble simulation of global mean surface warming.”

Page 3, Lines 15-16:

“In this study, we present a new method for combining the LGRTC approach with an arbitrary efficient Earth system model to generate computationally efficient local warming projections for arbitrary forcing scenarios.”

This change makes the revised manuscript more general in nature, and of interest to a wider range of readers.

**Point 2: Link to emissions budgets and regional impacts.** We agree that the approximation tool presented provides a useful link to assess regional impacts from carbon emissions/carbon budgets. In our revised manuscript we have improved this link by exploring the spatial warming pattern (the LGRTC) for the RCP2.6 scenario (Fig. 1a,d) – a scenario with strong mitigation and a high likelihood of meeting the Paris Climate Agreement goals.

*“p4 14-10: I am not sure if three scenarios that all show various rates of continually increasing warming are sufficient to make this conclusion. I would suspect that this does not hold for RCP2.6 where most models stabilise in temperature but regional patterns may continue to evolve. It would be good to show this. It would be helpful to see the 1pctCO2 scenarios for comparison in figure 1, also. (also relevant to p6 16-10)”*

**Scenarios with increasing warming and scenarios with stabilised warming.** We agree that the scenarios considered have increasing warming {although we note that in RCP4.5 there is little additional warming after 2080 across the 13 CMIP5 models considered by Goodwin et al., (2018b – see figure 2c therein, grey shaded area), we agree that there is little time for the warming pattern to continue to evolve}.

We also agree that the RCP2.6 scenario offers a chance to explore our LGRTC tool for generating local warming projections in a scenario with stabilised climate. In this revised version we produce a LGRTC for RCP2.6 (Fig. 1a,d) and compare this to the existing scenarios (Table 1). This allows us to test our methodology for a climate with warming stabilised close to the Paris Climate Agreement warming targets of 1.5 and 2.0 °C.

*“p4122: a point on different non-CO2 forcers in the three scenarios - the RCPs are quite heterogeneous in their aerosol forcing in future scenarios, and 1pctCO2 does not include them. I'm not sure this gives us much information for pattern scaling for custom emissions scenarios. See figure 3 in Liu et al. for temperature responses to - admittedly somewhat extreme - cases of aerosol forcing in Europe and Asia. <https://doi.org/10.1175/JCLI-D-17-0439.s1> . Some more discussion about how this model could handle widely varying timeseries of global and regional aerosol forcing would really help strengthen the model (and paper).”*

**Pattern scaling for custom emissions scenarios with extreme aerosol emissions.** Our analysis now demonstrates how a single LGRTC with small uncertainty covers both RCP4.5 and RCP8.5 scenarios (Fig. 2c,f,i), and so will also be applicable to similar scenarios. In the production of the RCP scenarios, assumptions have been made as to the relative amounts of different forcing agents emitted (e.g. CO<sub>2</sub>, other well mixed greenhouse gasses, aerosols etc) (e.g. see IPCC, 2013 or Meinshausen et al., 2011). Some forcing agents, specifically aerosols, are not well mixed in the

atmosphere but exert a significant local influence. We agree that for extreme cases of localised aerosol radiative forcing the pattern of warming would be different to the assumptions used in the generation of the different RCP scenarios.

In a revised manuscript, we state how our generic LGRTC approach can be applied to scenarios with similar underlying assumptions to the RCP scenarios (Page 6, Lines 33-35):

“The *generic*  $\geq 2^\circ\text{C}$  LGRTC pattern (Fig. 2) assumes idealised future pathways within the range of the RCP4.5 and RCP8.5 scenarios (Figure 3b,c), including a similar ratio of  $\text{CO}_2$  to non- $\text{CO}_2$  radiative forcing and spatial emissions of anthropogenic aerosols.”

We then also explain how our generic LGRTC approach cannot be applied to scenarios with extreme spatial aerosol forcing that differs widely from the RCOP scenarios (p. 6 Lines 35-37):

“This *generic*  $\geq 2^\circ\text{C}$  LGRTC field should not be used for extreme scenarios that differ widely from the underlying societal assumptions of the RCP scenarios, for example in their spatial aerosol forcing (e.g. see Liu et al., 2018).”

The method presented could potentially be extended in future work to attempt to calculate the impact on the LGRTC of different localised aerosol forcing patterns. For example by:

(1) Calculating the LGRTC for a scenario with  $\text{CO}_2$  only (or well mixed greenhouse gas only) forcing, (2) Exploring the sensitivity of LGRTC patterns to regional aerosol emission in complex climate models, for cases with idealised aerosol emissions for each region (e.g. Europe, Asia etc). (3) Combining the LGRTC from well mixed greenhouse forcing with the LGRTC from idealised aerosol forcing in each region, using knowledge of the relative emissions from greenhouse gasses and aerosols by region in the custom scenario, to generate a custom warming pattern for a scenario with extreme aerosol emission patterns. The key to such a method working is that the uncertainties introduced by the assumptions involved in combining different spatial patterns are smaller than the uncertainties introduced by the range of CMIP class model responses for a given scenario.

Since this potential method relies on new targeted experiments with complex CMIP models, this is not feasible to conduct for this paper and is reserved for future study.

Note that the calculations for the LGRTC presented here will apply for custom scenarios that do utilise similar assumptions to the RCP scenarios in terms of the relative amounts of well mixed greenhouse emissions and aerosols.

**Minor/stylistic points.** We also thank Dr. Smith for also raising minor/stylistic points, which we can confirm have all be addressed in the revised version.

## Reply to reviewer 2's comments

### *“1 General comments*

*Goodwin et al. present a tool for projecting local warming with uncertainty from multiple anthropogenic emissions scenarios. The major advance of the paper is the combination of output from a probabilistic climate model and warming ratios from AOGCM/ESMs (I note that the MAGICC/SCENGEN, <http://www.cgd.ucar.edu/cas/wigley/magicc/>, tool does a similar thing but given that this paper is not tightly coupled to MAGICC or any other probabilistic climate model and its code is open sourced I consider this paper to be a significant advance on the MAGICC/SCENGEN tool). I feel that this advance could be a very useful addition to the literature if a few concerns were addressed to provide more confidence in the paper's conclusions.”*

**General comments.** We are pleased the reviewer sees the advance offered, and in this revision we have amended the manuscript to address the specific concerns raised – please see details below.

*“My major concerns focus on: whether the tool is actually scenario specific or not, how uncertainties from the climate model and LGRTC are combined and whether WASP is actually a key part of the tool or whether any probabilistic climate model could be used.*

*One other key comment, given the availability of CMIP6 model output, I feel this paper could be significantly improved if it were to use CMIP6 output rather than focussing on CMIP5.”*

**Concerns.** We spell out in detail below how our revision addresses the concerns raised. In brief, the revised manuscript:

- (1) Analyses the LGRTC for an additional scenario, RCP2.6 (new Fig. 1a,d), and provides more robust statistical comparisons of the differences in LGRTC for the different scenarios (new Table 1; new Fig. 2), including identifying a spatial domain over which more generic LGRTC fields can be applied (Fig. 2a,b,c);
- (2) Stresses that the method is not specific to the WASP model, and makes it clear that our methodology can be applied to any efficient model generating projections of global mean surface warming (Changed title; plus e.g. Page 1 Lines 17-20); and
- (3) Reserves the analysis of CMIP6 model output for future study.

### *“2.1 Scenario specificity of pattern scaling*

*It is not clear to me that the pattern scaling technique here is actually scenario agnostic. All the presented results are scenario specific (the RCP45 projections use RCP45 LGRTC and the RCP85 projections use RCP85 LGRTC) and there is no analysis of whether a ‘general LGRTC’ can be used nor whether such a ‘general LGRTC’ would have small enough uncertainties as to be useful.”*

**Scenario specificity of the LGRTC.** We agree that the LGRTC pattern scaling technique is not truly scenario agnostic – there are of course factors about a scenario that affect the LGRTC. However, this revised version explores, by comparing the LGRTC for three RCP scenarios, how the LGRTC approach can be applied over scenarios that are similar to, yet not precisely the same as, the specific RCP scenarios.

*“I feel the comment (page 6, line 10), ‘This allows future users to choose the spatial pattern scaling that is most suitable for their scenario.’ is misleading. Only 3 patterns are available and none of them have been shown to be applicable for an emissions scenario different to the one from which they were derived (see comment above). Such cross-validation would be a vital step to providing confidence that the spatial pattern derived from one scenario can then be applied to any arbitrary scenario.”*

Agreed that the sentence “This allows future users to choose the spatial pattern scaling that is most suitable for their scenario’ was unclear, and this statement has been removed in the revised version. We now quantify how different the scenario LGRTC fields are, in terms of the ratio of inter-model variation to inter-scenario variation in the LGRTC (Table 1). We also combine the scenarios

Note that the arbitrary and generic  $\leq 2^{\circ}\text{C}$  LGRTC patterns (that include RCP2.6 information) are not practical to use because of the large uncertainties in the LGRTC, caused by the large inter-model differences in the RCP2.6 LGRTC patterns for CMIP5 models (Fig. 1d). However, for most of the globe the variation between CMIP5 model LGRTC patterns is still larger than the variation between scenarios (Fig. 2a,b – consider the regions with a valid domain). Therefore, the approach is valid for a large domain, it just results in high uncertainty.

See below for details on broader points.

*"I am not convinced by the comment (page 4, line 8), 'The absolute value of differences in LGRTC between the three scenarios was below 0.72C perC in all grid-cells and mostly below 0.2C perC over the continents. Therefore, the choice of the emission scenario to define spatial pattern of warming in this study is not much relevant when only inhabited regions are considered.' Relative to strong mitigation targets (e.g. the 1.5C target), I am not convinced these are trivial variations. In addition, in this context 'mostly' is meaningless and provides no quantification of how wide the disagreement is nor of the regions in which this generalisation doesn't hold (and how wrong it is)."*

*"I am also not convinced by the comment (page 4, line 19), 'This might have led to the large differences in the Arctic region, but detailed analysis and explanation is outside the scope of this study.' If the pattern scaling approach is to be used for arbitrary scenarios, there needs to be evidence that one pattern, with sufficiently large uncertainties, can be applied to multiple scenarios and give results that are in line with known results from CMIP models. Any differences need to be explained as they are of key interest when applying this tool (or the tools' domain of applicability should only be limited to those regions where the differences are small/well understood)."*

**Imprecise wording of comparisons between scenario-LGRTC patters.** Agreed that the highlighted sentences do not provide robust statistical analysis of the differences and similarities between the LGRTC patterns for the scenarios. In a revised manuscript, we now provide a robust statistical comparison of the LGRTC for different scenarios (Table 1) and over different areas of the domain (Figure 2g,h,i). We now define the domain over which the tool is applicable for more generic scenarios that are similar to, but not identical to, the RCP2.6, RCP4.5 and RCP8.5 scenarios. See answer to the next paragraph for more details.

*"I think the data is there to address this concern. One suggestion (which would satisfy me) would be to derive some 'general LGRTC' (including uncertainty) which could be used with any emissions scenario. The 'general LGRTC' could then be applied to the RCPs (here meaning all RCPs, including RCP26 and RCP60, not just RCP45 and RCP85) and the differences quantified. This would provide a meaningful quantification of how big the uncertainties need to be on a 'general LGRTC' for it to sufficiently capture the variation across CMIP models and scenarios in the cases where we have data. I would be even more convinced if a 'general LGRTC' derived from CMIP5 RCPs was shown to hold for CMIP6 SSP scenarios."*

**Addressing concern over applicability of LGRTC for different scenarios/scenario dependence quantification.** Agreed that greater insight into the amount of scenario-dependence is required, and that this affects the validity of using the LGRTC for scenarios other than the scenarios from which they were derived. The following changes improve the manuscript:

(1) The revised manuscript analyses the LGRTC for an additional scenario, RCP2.6 (a stabilisation scenario with strong mitigation in line with the Paris Climate Agreement's targets of keeping warming under 2.0 °C): Fig. 1a,d). This scenario shows greater inter-model variation (Fig.1d compared to Fig 1e,f). In part, this greater model variation in LGRTC will likely be due the lower global mean warming in the RCP2.6 scenario: since the LGRTC has the global mean warming on the demoninator, scenarios that have small global mean warming will likely show more variation in spatial LGRTC patterns for different models.

(2) The revised manuscript provides a meaningful statistical comparison of the LGRTC for the different scenarios (RCP8.5, RCP4.5 and RCP2.6: Table 1). This statistical comparison constitutes a comparison of the magnitudes of LGRTC uncertainty due to differences 'within scenario but between CMIP5 models' to the LGRTC differences 'between scenarios'. i.e. comparing  $\sigma_{\text{LGRTC}}$  within a scenario to the differences between  $\mu_{\text{LGRTC}}$  for different scenarios.

(3) The revised manuscript explores the feasibility of defining a domain over which a set of generic LGRTC patterns can be defined (with uncertainties large enough to capture variation across CMIP5 models and variation between scenarios).

Three generic LGRTC patterns are produced (Fig. 2): (i) an arbitrary scenario for any warming level (made by combining RCP2.6, RCP4.5 and RCP8.5); (ii) a generic scenario for warming up to 2 °C (made by combining RCP2.6 and RCP4.5); and (iii) a generic scenario for warming of 2 °C and more (made by combining RCP2.6 and RCP8.5).

The methods used to produce the generic LGRTC fields are explained in Section 3.2.1, including equations (2) and (3). Ultimately, a key property of a generic LGRTC pattern must be that the uncertainty introduced by the scenario choice is less than the uncertainty introduced by the range of CMIP-class model responses within each a given scenario. Therefore, the revised manuscript restricts the domains of the generic LGRTC patterns to locations where the condition  $|\mu_j - \mu_k|/\sigma_{LGRTC} < 1.0$  is met. This comparison also quantifies the value of  $|\mu_j - \mu_k|/\sigma_{LGRTC}$  over the globe (Fig. 2g,h,i).

We will reserve comparisons to CMIP6 for future study.

## “2.2 Scenario specificity of WASP

*WASP currently requires exogenous estimates of non-CO2 radiative forcing (see manuscript paragraph starting page 7, line 33). As far as I can tell, this means that this tool is not applicable to arbitrary emissions scenarios but rather only ones for which there is an available non-CO2 radiative forcing quantification. I feel this is a rather fatal flaw of a tool which is meant to be applicable to arbitrary emissions scenarios.*

*An easy remedy would be to alter the tool from being ‘WASP/LGRTC’ to ‘a general framework for coupling probabilistic climate model output and LGRTC’ (insert acronym here) i.e. remove the explicit dependence on WASP. I can’t see any reason why WASP is the only model with which this tool would work. This paper could still illustrate the use of the framework with WASP output, but such a reframing would make clear that the coupling could be done with any probabilistic climate model so a model which can run fully GHG-emissions driven could be used instead and would immediately fix the issue of WASP’s limited available scenario set.”*

Agreed, the method’s (non)reliance on WASP is now explicitly stated. We agree that the LGRTC method can be applied to any arbitrary probabilistic climate model ensemble, not just the WASP ensemble used in the study. We have reframed the manuscript title and text in terms of offering a general framework, with WASP the efficient model used as an example tool to illustrate the approach.

## “2.3 Combination of uncertainties

*I am not convinced that the combination of uncertainties in equation 2 is correct. In equation 2, shouldn’t the resulting distribution be the product/convolution of the two distributions rather than the output of random sampling from the two distributions? Given LGRTC is assumed to be gaussian, and that the WASP output is approximately gaussian, wouldn’t it be better to derive the distribution of Delta T\_i (x, y, t) by taking the product of two gaussians (see e.g. [https://ccrma.stanford.edu/~jos/sasp/Product\\_Two\\_Gaussian\\_PDFs.html](https://ccrma.stanford.edu/~jos/sasp/Product_Two_Gaussian_PDFs.html)) which isn’t the same as the product of two gaussian variables (see e.g. <https://math.stackexchange.com/questions/101062/is-the-product-of-twogaussian-random-variables-also-a-gaussian>). I’m happy to be corrected on this as I am not a statistical expert. However, regardless of whether I am correct or not I think some explanation must be added to the manuscript or the supplementary to explain this uncertainty propagation.”*

**Combination of uncertainties.** We agree with the statistical points made about the random sampling of two Gaussian distributions not in general giving the same answer as the convolution of two Gaussian distributions.

However, to make our LGRTC method applicable to any arbitrary probabilistic projection of global mean surface warming (not just from this WASP ensemble), we cannot assume that the projection of global mean surface warming is Gaussian. It may be that a projection of global mean surface warming is significantly skewed, for example due to a skewed probability distribution of climate sensitivity with a long tail of high values (e.g. see Assessment Report 5 of the IPCC, 2013). Therefore, to ensure that our approach is generally applicable to any efficient model's projection of global mean surface warming, we cannot take product of two Gaussian distributions as suggested by the reviewer. We explain this on Page 7 Lines 9-13:

“Note that eq. (2) does not assume that the distribution of global mean temperature projections,  $\Delta^-(T_i)(t)$ , from the efficient Earth system model is Gaussian. The distribution of  $\Delta^-(T_i)(t)$  may not be Gaussian if, for example, the assumed climate sensitivity distribution has a long tail of high values (e.g. see Knutti et al., 2017). Thus, this method for generating the local warming distribution, eq. (2), can be applied to any arbitrary distribution of global mean surface warming from any arbitrary efficient climate model.”

Our method, of randomly sampling from both the distributions of global mean warming and LGRTC, is applicable to any arbitrary projection of global mean surface warming from any arbitrary efficient Earth system model.

We now also point out that in the MATLAB approximation tool, which does tie in to the WASP ensemble, we have used the product of two Gaussian distributions (as the reviewer suggests) rather than random sampling (Page 8 Lines 26-27):

“Note that in this approximation tool the uncertainty in local warming is calculated directly by multiplying the assumed Gaussian distributions of LGRTC and global mean warming, eq. (8).”

#### *2.4 Reliance on WASP*

*It is not clear if this paper is using an existing WASP probabilistic distribution or presenting a new one (e.g. contradiction between page 5, line 9: ‘3x10<sup>6</sup> members’ and page 2, line 23: ‘10<sup>8</sup> simulations’). If the reframing suggested earlier were to take place then this is no longer an issue (as the choice of particular probabilistic climate model is just for illustration and isn’t a key feature of the tool). However, if this particular WASP probabilistic distribution is key then I would have to consider that component more closely.”*

**The (non)reliance on WASP.** The novel methodology (of combining the LGRTC with a probabilistic ensemble of global mean warming from an efficient numerical model) is not tied to WASP. Therefore, we will be making the reframing suggested by the reviewer earlier clear in a revised manuscript. We adopt the probabilistic ensemble generated in Goodwin et al (2018b). We will make the particular ensemble used clear in the revised manuscript.

We note that there is not a contradiction between having 3x10<sup>6</sup> members in the posterior ensemble and 10<sup>8</sup> members of the prior ensemble in the WASP methodology (see below).

*“(If the WASP probabilistic distribution is not key this entire paragraph can be ignored but for completeness) At the moment ...*

Our revised manuscript now presents a LGRTC method that can be applied to any efficient model's projection of global mean surface warming (rather than specific to only the WASP model). Therefore, the WASP probability distribution is not key to the manuscript's findings, and so the points made by the reviewer in this paragraph are not relevant – as the reviewer identified.

# A computationally efficient method for probabilistic local warming projections constrained by history matching and pattern scaling, demonstrated by WASP-LGRTC-1.0

Deleted: model

Deleted:

Philip Goodwin<sup>1</sup>, Martin Leduc<sup>2</sup>, Antti-Ilari Partanen<sup>3</sup>, H. Damon Matthews<sup>4</sup> and Alex Rogers<sup>5</sup>

<sup>1</sup>School of Ocean and Earth Science, University of Southampton, Southampton, SO14 3ZH, UK

<sup>2</sup>Ouranos, Montreal, Canada

<sup>3</sup>Climate System Research, Finnish Meteorological Institute, Helsinki, Finland

<sup>4</sup>Department of Geography, Planning and Environment, Concordia University, Montreal, Canada

<sup>5</sup>Department of Computer Science, University of Oxford, Oxford, UK

Correspondence to: Philip Goodwin (p.a.goodwin@soton.ac.uk)

**Abstract.** Climate projections are made using a hierarchy of models of different complexities and computational efficiencies. While the most complex climate models contain the most detailed representations of many physical processes within the climate system, both parameter space exploration and Integrated Assessment Modelling require the increased computational efficiency of reduced-complexity models. This study presents a computationally efficient method for generating probabilistic projections of local warming across the globe, using a pattern scaling approach derived from the Climate Model Intercomparison Project phase 5 (CMIP5) ensemble, that can be coupled to any efficient model ensemble simulation of global mean surface warming. First, global mean warming is projected using a 10<sup>3</sup>-member ensemble of history-matched simulations with an example reduced complexity Earth system model: the Warming Acidification and Sea-level Projector (WASP). The ensemble-projection of global mean warming from this WASP ensemble is then converted into local warming projections using a pattern scaling analysis from the CMIP5 archive, considering both the mean and uncertainty of the Local to Global Ratio of Temperature Change (LGRTC) spatial patterns from the CMIP5 ensemble for high-end and mitigated scenarios. The LGRTC spatial pattern is assessed for scenario dependence, in the CMIP5 ensemble using RCP2.6, RCP4.5 and RCP8.5, and spatial domains are identified where the pattern scaling is useful across a variety of arbitrary scenarios. The computational efficiency of our WASP/LGRTC model approach makes it ideal for future incorporation into an Integrated Assessment Model framework, or efficient assessment of multiple scenarios. We utilise an emergent relationship between warming and future cumulative carbon emitted in our simulations to present an approximation tool making local warming projections from total future carbon emitted.

Deleted: n efficient model

Deleted: for

Deleted: ing

Deleted: ,

Deleted: combining observation constrained global mean projections of an efficient Earth system model with spatial pattern scaling derived from the Climate Model Intercomparison Project phase 5 (CMIP5) ensemble.

Deleted: the

Deleted: Earth system model

Deleted: does not appear strongly

Deleted: scenario dependent

Deleted: so should be

Deleted: \*

## 1 Introduction

The dominant climate projections, used by the 5th Assessment Report (AR5) of the Intergovernmental Panel on Climate Change (IPCC, 2013), are made using the Climate Model Inter-comparison Project phase 5 (CMIP5) ensemble (Taylor et al, 2012). However, due to their high level of complexity, state-of-the-art CMIP5 Earth System Models (ESMs) are computationally demanding, and thus cannot be used on a regular basis to inform decision makers about the impacts of arbitrary carbon-emission scenarios.

While a couple of years separate the different generations of CMIP-like experiments, many applications rather require climate simulations to be generated within a much shorter time frame. For instance, impact assessments may require climate projections for scenarios not considered by the CMIP5 experiments, for example scenarios designed to meet Paris Climate Agreement targets and maintain global mean surface warming below 1.5 or 2 °C (e.g. van Vuuren et al., 2018; Brown et al., 2018; Nicholls et al., 2018; Goodwin et al., 2018a), and physical climate simulations are required within Integrated Assessment Models exploring the coupled economic, societal, ecological and climate systems (e.g. van Vuuren et al., 2018; van Vuuren et al., 2017; McJeon et al., 2014).

To generate computationally efficient climate simulations, a range of lower-complexity – but numerically more efficient – climate models have been developed. They generally use a reduced spatial resolution and/or a simplified representation of processes included within the complex models (e.g. Smith, 2012; Meinshausen et al., 2011a; Goodwin et al., 2018b).

5

For example, the highly efficient MAGICC6 climate model uses an upwelling-diffusion representation of the ocean and an hemispherical averaged spatial resolution (Meinshausen et al., 2011a). MAGICC6 has been configured to emulate an ensemble of the more complex Climate Model Intercomparison Project phase 3 (CMIP3) climate models (Meinshausen et al., 2011a; 2011b), but at a fraction of the computational expense. To generate spatial projections using MAGICC, a pattern scaling approach (e.g. Herger et al., 2015) is applied to emulate the spatial climate patterns from the CMIP3 models (e.g. Fordham et al. 2012): the regional climate SCENarioGENerator (SCENGEN). This MAGICC6 (and combined MAGICC6/SCENGEN) climate model is computationally efficient enough to usefully couple into Integrated Assessment Model (IAM) frameworks, including the IMAGE and MESSAGE frameworks (van Vuuren et al., 2017; McJeon et al., 2014). A key goal of IAMs is to explore consequences of the coupled human-climate system, through coupling representations of the physical climate system with the biosphere and human/society interactions, often including energy generation and land-use changes.

10

15

A recent study (Goodwin et al., 2018b) takes a different approach to making future projections of global mean surface warming, using the computationally efficient Warming Acidification and Sea-level Projector (WASP) climate model (Goodwin, 2016; Goodwin et al., 2017). In Goodwin et al. (2018b) the efficient WASP model is configured, not by tuning the parameters to emulate existing complex climate models (e.g. Meinshausen et al., 2011a; 2011b), but instead by history matching (Williamson et al., 2015) the efficient model to real world data. Goodwin et al. (2018b) first generate one hundred million ( $10^8$ ) simulations using WASP, by varying the model properties with a Monte Carlo approach. This includes an input distribution for climate sensitivity drawn from geological evidence (PALEOSENS, 2012). These  $10^8$  simulations are then integrated from year 1765 to 2017, and each of them is checked against a set of historic observational reconstructions of surface warming (Hansen et al., 2010; Smith et al., 2008; Vose et al., 2012), ocean heat uptake (Levitus et al., 2012; Giese et al., 2011; Balmaseda et al., 2013; Good et al., 2013; Smith et al., 2015; Cheng et al., 2017) and carbon fluxes (IPCC, 2013; le Quéré et al., 2016). Only those WASP simulations that are consistent with the observational constraints are extracted to form the final history-matched ensemble of around  $3 \times 10^4$  simulations (Goodwin et al., 2018b, see Supplementary Table 3 therein). This final history matched ensemble is then used to make future projections (Goodwin et al., 2018b). Note that the WASP ensemble is not configured to emulate the performance of more complex models, but to be consistent with observations of the real climate system.

20

25

30

The WASP model (Goodwin, 2016) produces projections for global mean surface warming only (Goodwin et al., 2018b), so to gain information to calculate local warming we here apply a pattern scaling tool. Leduc et al (2016) have recently shown that the spatial pattern of warming across CMIP5 models is relatively robust even though the average warming varies widely between ensemble members. Using the well-known pattern scaling approach (Tebaldi and Arblaster, 2014), Leduc et al. (2016) calculated the spatial pattern of the Local to Global Ratio of Temperature Change (LGRTC) that represented the CMIP5 ensemble, including both the mean and standard deviation in this spatial pattern.

35

40

Globally, the near-linear sensitivity of mean surface warming to cumulative carbon emissions is expressed via the Transient Climate Response to cumulative CO<sub>2</sub> Emissions (TCRE in °C per 1000PgC), which is estimated to be in the range 0.8 to 2.5 °C per 1000PgC (IPCC, 2013; Matthews et al, 2009). One approach to generating local warming projections from carbon

emission scenarios is to simply multiply the LGRTC characteristic of the CMIP5 ensemble (Leduc et al, 2016) by the estimated range for the TCRE and by the cumulative carbon emissions. However, this approach cannot be used to investigate or simulate several phenomena of potential interest. Firstly, the effective TCRE depends on the ratio of CO<sub>2</sub> to non-CO<sub>2</sub> radiative forcing (Williams et al. 2017a). Therefore, while the efficient climate models can be applied to investigate future warming for arbitrary scenarios, the TCRE cannot be applied unless it is for a scenario for which the TCRE is already estimated (e.g. Matthews et al. 2009; Williams et al., 2017a), for example the defined Representative Concentration Pathway (RCP) scenarios (Meinshausen et al. 2011c) or an idealised scenario with 1% per year increase in CO<sub>2</sub> concentration (1pctCO<sub>2</sub>; Taylor et al, 2012) and no other forcing. Secondly, studies indicate that there can be a period of continued surface warming following cessation of annual carbon emissions (Frölicher et al., 2014; Williams et al., 2017b). This phenomenon cannot be explored using the TCRE alone, but is represented within efficient climate models such as WASP (Williams et al., 2017b). Thirdly, there is evidence that in some circumstances there is a path-dependence of surface warming from cumulative emissions (Zickfeld et al, 2012), for example where cooling following negative emissions may not re-trace the previous warming pathway. Again, this phenomenon is not captured within a constant TCRE framework, but may be explored with climate models. Thus a TCRE framework is applicable for certain situations, including idealised scenarios where the TRCE has already been established, but in the general case a time-dependent Earth system model is required.

In this study, we present a new method for combining the LGRTC approach with an arbitrary efficient Earth system model to generate computationally efficient local warming projections for arbitrary forcing scenarios. Using the WASP model as our example efficient Earth system model. The combined WASP/LGRTC model makes local warming projections that are history matched to constrain the global mean surface warming (Goodwin et al., 2018b) and pattern scaled to the CMIP5 ensemble to generate the local information (Leduc et al., 2016). Our efficient method of ensemble generation is able to produce warming-projections to year 2100 for arbitrary future carbon-emission scenarios in a matter of seconds on a standard desktop computer (with the computational efficiency of the particular, WASP, efficient model used). An approximation tool is also presented making local warming projections based on future cumulative carbon emitted, for idealised scenarios where the TCRE has been pre-established.

Deleted: combined WASP/LGRTC Earth system model

Deleted: T

Deleted: model

Section 2 describes the spatial warming patterns analysed for RCP4.5 (Thomson et al., 2011) and RCP8.5 (Riahi et al., 2011) scenarios in 22 CMIP5 models, following the methodology of Leduc et al. (2016). Section 3 describes our methods for producing an ensemble of warming projections for any locality using the combined WASP/LGRTC Earth system model, while Section 4 presents the approximation approach for cases when the TCRE is pre-established. Section 5 discusses the wider implications of this study.

Deleted: r

## 2. Spatial warming patterns in the CMIP5 ensemble for RCP2.6, RCP4.5 and RCP8.5

Leduc et al (2016) demonstrated the utility of considering the spatial warming over time as a product of the global mean warming,  $\Delta\bar{T}(t)$ , and the spatial pattern of the Local to Global Ratio of Temperature Change, LGRTC( $x,y$ ), in the CMIP5 ensemble,

$$\Delta T(x, y, t) = \Delta\bar{T}(t) \times \text{LGRTC}(x, y). \quad (1)$$

The mean and standard deviation in LGRTC were analysed across 12 CMIP5 models (Leduc et al, 2016), under a 1 per cent per year increase in atmospheric CO<sub>2</sub> concentration (1pctCO<sub>2</sub>; Taylor et al, 2012). To first order, the mean LGRTC can be treated as being independent of time and emission scenarios (Leduc et al, 2016, 2015).

Here, the spatial warming patterns in 22 CMIP5 models (see Supplementary Table S1) are examined for RCP4.5 (Thomson et al., 2011) and RCP8.5 (Riahi et al., 2011) scenarios that contain also non-CO2 forcings from for example anthropogenic non-CO2 greenhouse gas and aerosol emissions. We evaluated the LGRTC comparing mean global temperature between years 2006-2025 and 2079-2098. RCP2.6 data was not available for models CESM1-BGC, Inmcm4, and IPSL-CM5B-LR.

5 For the other 19 models, we calculated the RCP2.6 LGRTC for the temperature peak period, defined as a 20-year time window with the maximum time-average global mean surface air temperature. Different models had the peak temperature at different times so the we identified the peak individually for each model run. For most models, the peak in 20-year running-mean global temperature was around year 2070. For MIROC-ESM, CSIRO-Mk3-6-0, CCSM4, MRI-CGCM3, and CSIRO-Mk3-6-0 the period with the highest mean temperature was the years 2079-2098. The same reference period (2006-2025)  
10 was used as with the calculation of LGRTC using the end-of-the-century period for RCPs 4.5 and 8.5. Note that for RCP2.6 the LGRTC was calculated using the peak temperature period, rather than 2079-2098, because the 2078-2098 period was a similar temperature, or colder, than 2006-2025 in some models, making the calculation of LGRTC impractical since the denominator of the calculation (the global mean temperature change) was too small or negative.

15 Figure 1 shows the multi-model mean LGRTC ( $\mu_{LGRTC}$ ) and multi-model standard deviation in LGRTC ( $\sigma_{LGRTC}$ ) for the RCP4.5, RCP8.5 and RCP2.6 scenarios. With exception of oceanic regions where non-linear processes have important impacts on the climate sensitivity, such as the sea-ice albedo feedback in the Arctic and the meridional overturning circulation in the north Atlantic (Leduc et al., 2016), LGRTC is very similar in the RCP4.5 and RCP8.5 scenarios (Fig. 1, b,c). The uncertainty of the warming patterns within each scenario, defined as standard deviation of LGRTC within the  
20 model ensemble ( $\sigma_{LGRTC}$ ), was largest in the Arctic Ocean and in the Southern Ocean for RCP4.5 and RCP8.5 (Fig 1e,f). The spatial average of the multi-model standard deviation was larger in the RCP4.5 than in RCP8.5 over most areas of the globe. Over continents, it was around 0.15-0.45 in RCP4.5 and mostly below 0.3 in RCP8.5. The RCP2.6 scenario shows greater multi-model mean LGRTC at low latitudes (Fig. 1a,b,c), and has more inter-model variation in the LGRTC at high latitudes (Fig. 1, d,e,f), compared to the RCP4.5 and RCP8.5 scenarios.

25 The difference in LGRTC between two scenarios, relative to the multi-model variation within a scenario, is expressed via a spatially averaged ratio of  $[\mu_{LGRTC,i}(x,y) - \mu_{LGRTC,j}(x,y)] / \sigma_{LGRTC,i}(x,y)$ , where  $i$  signifies the reference scenario and  $j$  the scenario for comparison. Table 1 expresses how many multi-model standard deviations each of the three scenarios multi-model mean LGRTC lies relative to the other scenarios. Considering the mid-range scenario (RCP4.5) as the reference, the LGRTC for RCP8.5 lies a spatial average of just 0.17 standard deviations away from RCP4.5 (Table 1), indicating that the variation in LGRTC between models within the RCP4.5 scenario is more significant than the variation between RCP4.5 and RCP8.5 scenarios. In contrast, the LGRTC for the RCP2.6 scenario lies 2.8 standard deviations away from RCP4.5 (Table 1). The multi-model-mean LGRTC for RCP4.5 and RCP8.5 scenarios lie a spatial average of 0.78 and 0.75 standard deviations away from the RCP2.6 scenario respectively (Table 1). Note that the asymmetry in Table 1, with lower difference when RCP2.6 is used as the reference scenario, reflects the larger values of  $\sigma_{LGRTC}$  in the RCP2.6 scenario (Fig. 1d,e,f).

### 3 Local warming projections in the pattern-scaled WASP/LGRTC ensemble

The aim here is to generate computationally efficient future projections of local warming across the globe, including a measure of the uncertainty in those local warming projections. This is distinct from generating a spatial warming projection  
40 that is internally physically consistent, maintaining physically plausible teleconnections between warming at different locations. Each CMIP5 model simulation creates a unique internally physically consistent spatial warming pattern for the prescribed forcing. When projecting local warming, including a measure of uncertainty, one method is to use information on the average and variation in the LGRTC information from multiple CMIP5 models (Figs. 1, 2). However, as soon as the

Deleted: and

Deleted: like

Deleted: The absolute value of differences in LGRTC between the three scenarios was below 0.72 °C per °C in all grid-cells and mostly below 0.2 °C per °C over the continents. Therefore, the choice of the emission scenario to define spatial pattern of warming in this study is not much relevant when only inhabited regions are considered.¶

Deleted: Despite that the choice of the scenario has a relatively small impact on the warming patterns of interest here, it is worth noting that – in addition to the climate response to different radiative forcings – there are supplementary reasons explaining the previous differences. In particular, the differences in LGRTC between 1pctCO2 and the RCPs were caused by the lack of a clear basis for comparison: on the one hand, 1pctCO2 is an idealized scenario with no equivalent climatic states in the RCPs. For simplicity, we have chosen the preindustrial climate as the reference period in 1pctCO2 while in the RCP scenarios we used beginning of the 21st century. The end period was 20 years around the time of doubling of atmospheric CO2 concentration (70 years from the beginning) in 1pctCO2 and the years 2079-2098 in the RCPs. The different reference period meant that Arctic sea ice was already partly melted in the RCPs. This might have led to the large differences in the Arctic region, but detailed analysis and explanation is outside the scope of this study. Further differences between the 1pctCO2 scenario and the RCPs might have arisen from the different model ensemble. Both the different reference period and inclusion of non-CO2 forcings in RCP scenarios make the warming patterns from RCP scenarios more usable than those from the 1pctCO2 scenario to be used to predict warming patterns in the 21st century.¶

information from multiple CMIP5 models are combined, the averaged result may not be internally physically consistent in terms of the spatial pattern of warming.

Section 3.1 describes how an observation-constrained projection of global mean surface warming is generated, including uncertainty. Section 3.2 then combines this global mean projection with the LGRTC information from the CMIP5 models (Section 2, above) to generate local warming projections.

### 3.1 Generating global mean warming projections

The WASP Earth system model comprises an 8-box representation of carbon and heat fluxes between the atmosphere, ocean and terrestrial systems (Goodwin, 2016), with surface warming solved via a functional equation linking warming to cumulative carbon emitted (Goodwin et al, 2015). For the terrestrial system, carbon uptake by photosynthesis is dependent on temperature and CO<sub>2</sub>, while carbon release via respiration is temperature dependent. Heat and carbon initially enters the ocean at the surface ocean mixed layer. Once in the surface ocean mixed layer, heat and carbon are exchanged with the sub-surface ocean regions over e-folding timescales that vary between each simulation in the ensemble.

Here, the WASP model configuration of Goodwin et al. (2018b) is used. First, WASP is used to generate  $3 \times 10^6$  initial simulations in a Monte Carlo approach, each one integrated from years 1765 to 2017. A history matching approach (Williamson et al., 2015) is then adopted to assess these initial  $3 \times 10^6$  simulations for observational consistency against historic warming, ocean heat uptake and carbon fluxes (Supplementary Table S2; and see Goodwin et al., 2018b for how the history matching approach is applied to the WASP model). A total of  $1 \times 10^3$  simulations are found to be observationally consistent, such that their simulated values of surface warming, ocean heat uptake and carbon fluxes are consistent within observational uncertainty (Supplementary Table S2; Goodwin et al., 2018b).

The  $1 \times 10^3$  observation-consistent simulations are extracted to form the final history matched ensemble. This ensemble is then integrated into the future to generate the distribution of global mean surface warming over time, (Figure 3). The distributions of global mean surface warming,  $\Delta \bar{T}_i(t)$ , projected by this configuration and history matching approach using the WASP ensemble, are similar to the CMIP5 projections from highly complex ESMs for the four RCP scenarios (Goodwin et al., 2018b, see figure 2 therein). However, possibly because the WASP projections are more tightly constrained to observations, they show reduced ensemble spread in future warming compared to the CMIP5 ensemble.

### 3.2 Generating local warming projections

We now utilise projected distributions from the same configuration of the WASP model to calculate distributions of local warming across the globe using the LGRTC pattern scaling approach of Leduc et al (2016). The aim is to generate an ensemble of projections of local warming at time  $t$  for ~~some~~ scenario,  $\Delta T_i(x, y, t)$ , by using the history matched WASP projections of  $\Delta \bar{T}_i(t)$ , and the mean and standard deviation of the LGRTC for the CMIP5 models,  $\mu_{LGRTC}(x, y)$  and  $\sigma_{LGRTC}(x, y)$  respectively (Figs 2-3).

Deleted: a given RCP

#### 3.2.1 Constructing the LGRTC suitable for a range of non-RCP scenarios

The aim here is to apply a LGRTC calculation that will likely apply for multiple potential future scenarios, not just the three RCP scenario evaluated (Figure 1). To achieve this, we now combine the LGRTC fields for the different RCP scenarios to find aggregated LGRTC fields, considering the spatial domain over which this is likely to be feasible. The mean and standard deviations for the LGRTC at location  $x, y$ , in the new combined scenarios are calculated from the underlying RCP scenarios, using

$$\mu_{LGRTC}(x, y) = \sum_{i=1}^n \mu_i(x, y) / n \quad (2)$$

and

$$\sigma_{LGRTC}(x, y) = \sqrt{\sum_{i=1}^n (\sigma_i(x, y))^2} \quad (3)$$

where  $n$  is the number of underlying RCP scenarios used.

The domain of the LGRTC in the new combined scenarios is assumed valid where the variation in LGRTC between underlying RCP scenarios is less than the variation ascribed within the new scenario,  $\sigma_{LGRTC}(x, y)$ . This is calculated such that  $\mu_{LGRTC}(x, y)$  exists where the variation between the mean of the LGRTC from the different scenarios is less than the combined standard deviation in the LGRTC,  $|\mu_j - \mu_k| / \sigma_{LGRTC} < 1.0$ , for all combinations of two underlying RCP scenarios  $j$  and  $k$ .

This method (eqs. 2 and 3) is used to generate LGRTC fields for three potential generic scenarios (Figure 2). First, a scenario for any arbitrary future warming scenario (*arbitrary* scenario) is constructed by combining all three RCP scenarios (RCP2.6, RCP4.5 and RCP8.5) (Fig. 2a, d, g). Second, a LGRTC scenario for warming consistent with Paris Climate Agreement targets of 1.5 and 2 °C (*generic*  $\leq 2^\circ\text{C}$  scenario) is constructed by combining RCP2.6 and RCP4.5 (Fig. 2, b,e,h), the two RCP scenarios containing (at least some) model simulations that do comply with the Paris Agreement. Lastly, a LGRTC scenario for future warming that is likely to exceed the Paris Climate Agreement targets (*generic*  $\geq 2^\circ\text{C}$  scenario) is constructed using RCP4.5 and RCP8.5 (Fig. 2, c,f,i), the scenarios where most (RCP4.5) or all (RCP8.5).

The *arbitrary* and *generic*  $\leq 2^\circ\text{C}$  LGRTC scenarios are problematic to use in practice. Firstly, the large values of  $\sigma_{LGRTC}(x, y)$  across many regions, especially over land (Fig. 2d,e), make any local warming projection highly uncertain. The high  $\sigma_{LGRTC}(x, y)$  values arise from the high inter-model variation in the LGRTC in the RCP2.6 scenario (Fig. 1b, eqs. 2,3). Secondly, both *arbitrary* and  $\leq 2^\circ\text{C}$  generic scenarios have regions that fail the validity criteria,  $|\mu_j - \mu_k| / \sigma_{LGRTC} < 1.0$ , and so are outside of the prescribed LGRTC domains (Fig. 2a,b, white regions). The largest of these regions lie in the low latitude oceans, with most areas outside the valid domain being marine. Most densely populated areas on land are within the valid domain, and so the LGRTC approach can be applied to project future local warming. Areas outside the applicable domain (Fig. 2a,b) are generally where inter-model variation,  $\sigma_{LGRTC}(x, y)$ , is small (Fig. 2d,e and Fig. 1d,e,f), rather than where inter RCP scenario variation,  $\mu_j - \mu_k$ , is large (Fig. 1, a,b,c).

The *generic*  $\geq 2^\circ\text{C}$  LGRTC pattern, a combination of RCP4.5 and RCP8.5 (eqs. 2,3) is usable in practice for more generic future warming scenarios. The *generic*  $\geq 2^\circ\text{C}$  LGRTC pattern retains a small  $\sigma_{LGRTC}(x, y)$  (Fig. 2 compare f to d,e) and, due to the similarities between LGRTC fields for RCP4.5 and RCP8.5 scenarios (Fig. 1, Table 1), the LGRTC pattern for the *generic*  $\geq 2^\circ\text{C}$  scenario remains within the validity criteria for the entire globe (Fig. 2c,f,i). The *generic*  $\geq 2^\circ\text{C}$  LGRTC pattern (Fig. 2) assumes idealised future pathways within the range of the RCP4.5 and RCP8.5 scenarios (Figure 3b,c), including a similar ratio of CO<sub>2</sub> to non-CO<sub>2</sub> radiative forcing and spatial emissions of anthropogenic aerosols. This *generic*  $\geq 2^\circ\text{C}$  LGRTC field should not be used for extreme scenarios that differ widely from the underlying societal assumptions of the RCP scenarios, for example in their spatial aerosol forcing (e.g. see Liu et al., 2018).

### 3.2.2 Combining the LGRTC patterns with a probabilistic ensemble for global mean warming

Here, we combine LGRTC patterns (Figs. 1, 2) with global mean warming projections from an efficient Earth system model. While we use the WASP model here, other efficient models could be used. For the  $i$ th ensemble member of this history matched WASP ensemble, the WASP/LGRTC projection of local warming at location  $x, y$ ,  $\Delta T_i(x, y, t)$ , is constructed using both the mean and standard deviation in the LGRTC from the CMIP5 models,

$$\Delta T_i(x, y, t) = \Delta \bar{T}_i(t) \times [\mu_{LGRTC}(x, y) + z_i \sigma_{LGRTC}(x, y)], \quad (4)$$

where  $z_i$  is randomly chosen from a standard normal distribution. This distribution of local warming at time  $t$ , (eq. 4), includes both the uncertainty in global mean warming in the WASP ensemble (Figure 3; Goodwin et al., 2018b), and uncertainty in the spatial pattern of warming,  $\sigma_{LGRTC}$ , which is statistically derived from the CMIP5 ensemble (Figure 2; Leduc et al., 2016). Note that eq. (2) does not assume that the distribution of global mean temperature projections,  $\Delta \bar{T}_i(t)$ , from the efficient Earth system model is Gaussian. The distribution of  $\Delta \bar{T}_i(t)$  may not be Gaussian if, for example, the assumed climate sensitivity distribution has a long tail of high values (e.g. see Knutti et al., 2017). Thus, this method for generating the local warming distribution, eq. (2), can be applied to any arbitrary distribution of global mean surface warming from any arbitrary efficient climate model. If, however, the distribution of global mean surface temperature,  $\Delta \bar{T}_i(t)$ , were known in advance to be Gaussian, then it may be preferable to generate the local warming distribution,  $\Delta T_i(x, y, t)$ , by multiplying the Gaussian distributions for global warming and LGRTC directly, rather than applying eq. (2) which multiplies the individual values within each distribution.

The full WASP/LGRTC-ensemble local warming projections for RCP 4.5 and RCP 8.5 are given in Fig. 4, which shows the mean, 17th and 83rd percentile of the warming across the globe from the  $1 \times 10^3$  WASP/LGRTC ensemble members. To generate the local projections (eq. 4) for RCP4.5 and RCP8.5, we apply the pattern scaling analysed from the CMIP5 models for the appropriate scenario (Fig. 2). In both scenarios, there is more uncertainty, that is a higher range of responses between the 17th and 83th percentiles, in local warming at high northern latitudes (Fig. 4), consistent with this area showing a larger ensemble spread between CMIP5 models (Fig. 1).

The radiative forcing from aerosols can be highly localised, and so the ensemble mean and variation of local warming,  $\mu_{LGRTC}(x, y)$  and  $\sigma_{LGRTC}(x, y)$  in eq. (4), depends on how the CO<sub>2</sub> and non-CO<sub>2</sub> agents evolve in the scenario. For that reason, we include local warming patterns for the 1pctCO2 scenario as well as the RCP4.5, RCP8.5 and generic  $\geq 2^\circ\text{C}$  scenarios in the pattern scaling for the WASP/LGRTC model code (<https://doi.org/10.5281/zenodo.3819894>). This allows future users to choose the spatial pattern scaling that is most suitable for their scenario. The next section utilises the generic  $\geq 2^\circ\text{C}$  LGRTC pattern (Fig. 2c) to project spatial warming patterns for scenarios where the cumulative carbon emission is specified.

### 4. Approximation for arbitrary cumulative carbon emission scenarios

This section explores further increasing the computational efficiency for making spatial warming projections for idealised future scenarios, by approximating to the history matched WASP ensemble projections of global mean surface warming as function of cumulative carbon emitted after 2018,  $I_{em}$  in PgC.

The distribution of global mean surface warming in the WASP/LGRTC ensemble is approximately normally distributed for the RCP scenarios (Figure 3a). The history matched ensemble mean and standard deviation,  $\mu_{\Delta \bar{T}}$  and  $\sigma_{\Delta \bar{T}}$  respectively, are

Deleted: 2

Deleted: 2

Deleted: 2

Deleted: <https://doi.org/10.5281/zenodo.3446023>.

both well approximated by second order polynomials in cumulative carbon emitted (Figure 3b,c). The ensemble mean warming projections is given by,

$$\mu_{\Delta T}(I_{em}) = a_1 I_{em}^2 + b_1 I_{em} + c_1, \quad (5)$$

and the ensemble standard deviation by,

$$\sigma_{\Delta T}(I_{em}) = a_2 I_{em}^2 + b_2 I_{em} + c_2, \quad (6)$$

where  $a_1=3.50257 \times 10^{-7}$ ,  $b_1=2.50924 \times 10^{-3}$ ,  $c_1=1.02159$ ,  $a_2=2.14129 \times 10^{-8}$ ,  $b_2=2.28077 \times 10^{-4}$  and  $c_2=8.79361 \times 10^{-2}$  for RCP8.5. Both the RCP4.5 and RCP2.6 scenarios see very similar warming per unit future carbon emitted to RCP8.5, while the RCP6.0 scenario sees only slightly less warming per unit future carbon emitted (Figure 3b,c).

Therefore, for emission scenarios over the 21st century in which the ratio of radiative forcing from sources other than CO2 to cumulative carbon emitted during the 21st century lies within the range of the RCP scenarios, the distribution of global mean surface warming from the history matched WASP ensemble can be approximated by quadratics in future carbon emitted (eqs. 5 and 6; Fig. 3)

The mean warming at location  $x,y$  is calculated by simply multiplying the mean of the  $1 \times 10^3$  WASP ensemble members of the global average warming by the CMIP5 mean of the LGRTC,

$$\mu_{\Delta T}(x, y, I_{em}) = \mu_{\Delta T}(I_{em}) \times \mu_{LGRTC}(x, y). \quad (7)$$

The standard deviation in local warming at location  $x,y$  after cumulative emissions  $I_{em}$ ,  $\sigma_{\Delta T}(x, y, I_{em})$ , is then calculated from the standard deviation in the global average warming in the  $i$  ensemble members,  $\sigma_{\Delta T}(I_{em})$ , and the standard deviation in the LGRTC,  $\sigma_{LGRTC}(x,y)$ , using,

$$\sigma_{\Delta T}(x, y, I_{em}) = \mu_{\Delta T}(x, y, I_{em}) \sqrt{\left(\frac{\sigma_{\Delta T}(I_{em})}{\mu_{\Delta T}(I_{em})}\right)^2 + \left(\frac{\sigma_{LGRTC}(x,y)}{\mu_{LGRTC}(x,y)}\right)^2}. \quad (8)$$

Note that in this approximation tool the uncertainty in local warming is calculated directly by multiplying the assumed Gaussian distributions of LGRTC and global mean warming, eq. (8). This is unlike the uncertainty calculation for the generic method, eq. (4), which does not assume a Gaussian distribution for global mean warming. Applying equations (7) and (8) provides a method to approximate local warming projections as a function of the future carbon emitted after the start of 2018 (Figure 5a; code available at <https://doi.org/10.5281/zenodo.3819894>), including uncertainty in the warming at any location (Figure 5b). This method assumes idealised future pathways within the ranges of the RCP4.5 and RCP8.5 scenarios (Figure 3b,c), including a similar ratio of CO2 to non-CO2 radiative forcing. The generic  $>2^\circ\text{C}$  scenario LGRTC field (Fig. 2) is applied (Fig. 4), and as such the approximation tool should be utilised for cumulative carbon emission values that give a best estimate for global mean warming of  $2^\circ\text{C}$  or more. While this approximation tool (Fig. 5; eqs. 5-8) is not as general as the full WASP/LGRTC Earth system model in its potential applications, we anticipate it will still be a useful tool for back-of-the-envelope approximations and pedagogical applications.

Deleted: 3

Deleted: 4

Deleted: 4

Deleted: 3

Deleted: 4

Deleted: 5

Deleted: 6

Deleted: 5

Deleted: 6

Deleted: <https://doi.org/10.5281/zenodo.3446023>

Deleted: e RCP2.6,

Formatted: Font: Italic

Deleted: 3

Deleted: 6

Deleted: user-friendly

## 5. Discussion

A highly computationally efficient Earth System Model has been presented for projecting local warming projections, based on a history matched global mean warming projection using an efficient ESM (Goodwin, 2016; Goodwin et al., 2018b) and pattern scaling of the CMIP5 ensemble (Leduc et al., 2016): the WASP/LGRTC model. Along with the full WASP/LGRTC model is an easy to use normal error propagation approximation variant producing projected ranges of both global mean warming and the spatial distribution of warming for future cumulative carbon-emission values.

The WASP/LGRTC model presented here is an alternative to existing efficient climate models. For example, the MAGICC6/SCENGEN efficient model is often configured as an ‘emulator’ of the CMIP3 ensemble (Meinshausen et al, 2001a,b): the MAGICC6/SCENGEN model parameters are tuned such that the ensemble members emulate the properties of the more complex CMIP3 models in both global mean warming and spatial warming patterns. However, even the most complex of climate model ensembles show discrepancy to observations (Goodwin et al, 2018b), and this discrepancy will be reproduced by an emulating ensemble. In contrast, the WASP/LGRTC model is not tuned to emulate more complex models. Instead the WASP model parameters are empirically constrained using the observed histories of warming, heat uptake and carbon fluxes to generate global mean surface warming projections (Goodwin et al, 2018b). Meanwhile, the LGRTC spatial pattern applies the mean and standard deviation in the spatial warming from across the CMIP5 ensemble (Leduc et al, 2016), but does not seek to emulate any specific CMIP5 model within any specific WASP/LGRTC ensemble member.

At present, the WASP model requires prescribed radiative forcing from greenhouse gasses and agents other than CO<sub>2</sub>, for example methane or aerosols (Goodwin, 2016; Goodwin et al. 2018b). Future work will seek to implement an emission-based representation of other significant greenhouse gases and aerosols, allowing the WASP/LGRTC model to explore a wider range of future scenarios.

Both the WASP/LGRTC model and the quadratic approximation to WASP/LGRTC model are easy to use. The full WASP/LGRTC model can quickly generate output for arbitrary future scenarios, while the approximated model makes projections for different future cumulative emissions assuming that the relative CO<sub>2</sub> and non-CO<sub>2</sub> radiative forcing is in the range of the RCP8.5, RCP4.5 or RCP2.6 scenarios (Figure 3b,c compare black dashed line to red, orange and purple).

We anticipate that our full and approximated models will be beneficial both for scientific and pedagogical applications, where available computational resources or climate-model expertise exclude the use of highly complex models

**Code availability.** Versions of the WASP model is available from the public GitHub repository at [https://github.com/WASP-ESM/WASP\\_Earth\\_System\\_Model](https://github.com/WASP-ESM/WASP_Earth_System_Model). The specific code for both the WASP/LGRTC combined model approach used in this study, and the local warming projection approximation tool, are archived on Zenodo (<https://doi.org/10.5281/zenodo.3819894>).

Deleted: <https://doi.org/10.5281/zenodo.3446023>

**Author Contributions.** PG conducted the numerical modelling and coded the WASP/LGRTC model and approximation tool, with input from AR. AIP, MD and HDM analysed the spatial patterns in the CMIP5 models, and supplied the spatial arrays used by the WASP/LGRTC model and approximation tool. All authors contributed to writing the manuscript.

**Competing interests.** Authors declare no competing interests

**Acknowledgements.** PG acknowledges funding from UK NERC grant NE/N009789/1 and combined UK Government Department of BEIS and UK NERC grant NE/P01495X/1. ML thanks Ouranos and Concordia University. AIP was supported by Emil Aaltonen Foundation, The Fonds de recherche du Quebec - Nature et technologies (grant number: 200414), Concordia Institute for Water, Energy and Sustainable Systems (CIWESS), and Academy of Finland (grant number: 308365). We acknowledge the World Climate Research Programme's Working Group on Coupled Modelling, which is responsible for CMIP, and we thank the climate modelling groups (listed in Supplementary Table S1) for producing and making available their model output. For CMIP the U.S. Department of Energy's Program for Climate Model Diagnosis and Intercomparison provides coordinating support and led development of software infrastructure in partnership with the Global Organization for Earth System Science Portals.

10

#### References

Balmaseda, M. A., Mogensen, K., and Weaver, A. T.: Evaluation of the ECMWF ocean reanalysis system ORAS4. *Q. J. Roy. Meteorol. Soc.* 139, 1132–1161, 2013.

15 Brown, S., R. Nicholls, P. Goodwin, I. Haigh, D. Lincke, A. Vafeidis, J. Hinkel: Quantifying Land and People Exposed to Sea-Level Rise with No Mitigation and 1.5 and 2.0 °C Rise in Global Temperatures to Year 2300, *Earth's Future*, doi:10.1002/2017EF000738, 2018.

Cheng, L. et al.: Improved estimates of ocean heat content from 1960 to 2015. *Sci. Adv.* 3, e1601545, 2017.

20

Fordham, D.A., Wigley, T.M.L., Watts, M.J., and Brook, B.W.: Strengthening forecasts of climate change impacts with multi-model ensemble averaged projections using MAGICC/SCENGEN 5.3, *Ecography* 35, 4–8, doi:10.1111/j.1600-0587.2011.07398.x, 2012.

25 Frölicher, T. L., Winton, M., and Sarmiento, J. L.: Continued global warming after CO<sub>2</sub> emissions stoppage. *Nature Climate Change*, 4, 40–44, 2014

Giese, B. S., and Ray, S.: El Niño variability in simple ocean data assimilation (SODA), 1871–2008. *J. Geophys. Res.* 116, C02024, 2011.

30

Good, S. A., Martin, M. J., and Rayner, N. A.: EN4: quality controlled ocean temperature and salinity profiles and monthly objective analyses with uncertainty estimates. *J. Geophys. Res. Ocean.* 118, 6704–6716, 2013.

35 Goodwin, P., Brown, S., Haigh, I. Nicholls, R., and Matter, J.: Adjusting Mitigation Pathways to stabilize climate at 1.5 and 2.0 °C rise in global temperatures to year 2300, *Earth's Future*, doi:10.1002/2017EF000732, 2018a.

Goodwin, P., Katavouta, A., Roussinov, V.M., Foster, G.L., Rohling, E.J. and Williams, R.G.: Pathways to 1.5 and 2 °C warming based on observational and geological constraints, *Nature Geoscience*, doi:10.1038/s41561-017-0054-8, 2018b.

40 Goodwin, P.: How historic simulation-observation discrepancy affects future warming projections in a very large model ensemble, *Climate Dynamics*, doi:10.1007/s00382-015-2960-z, 2016.

Goodwin, P., Williams, R.G., and A. Ridgwell, A.: Sensitivity of climate to cumulative carbon emissions due to compensation of ocean heat and carbon uptake, *Nature Geoscience*, 8, 29-34, 2015.

Hansen, J., Ruedy, S., Sato, M., and Lo, K.: Global surface temperature change. *Rev. Geophys.* 48, RG4004, 2010.

5 Heger, N., Sanderson, B.M., and Knutti, R.: Improved pattern scaling approaches for the use in climate impact studies, *Geophys. Res. Lett.*, 42, 3486-3494, doi:10.1002/2015GL063569, 2015.

IPCC Climate Change 2013: The Physical Science Basis (eds Stocker, T. F. et al.) (Cambridge Univ. Press, Cambridge, 10 2013).

[Knutti, R., Rugenstein, M.A.A., and Hegerl, G.C., Beyond equilibrium climate sensitivity, \*Nature Geoscience\* 10, 727-736, 2017.](#)

15 Leduc, M., Matthews, H. D., and de Elía, R.: Quantifying the limits of a linear temperature response to cumulative CO2 emissions. *Journal of Climate*, 28(24), 9955–9968, 2015.

Leduc, M., Matthews, H.D., and de Elía, R.: Regional estimates of the transient climate response to cumulative CO2 emissions, *Nature Climate Change*, doi:10.1038/nclimate2913, 2016.

20 le Quéré, C. et al. Global carbon budget 2016. *Earth Syst. Sci. Data* 8, 605–649. 2016.

Levitus, S. et al.: World ocean heat content and thermosteric sea level change (0–2000 m), 1955–2010. *Geophys. Res. Lett.* 39, 10, 2012.

25 [Liu, L., Shawki, D., Voulgarakis, A., Kasoar, M., Samset, B.H., Myhre, G., Forster, P.M., Hodnebrog, Ø., Sillmann, J., Aalbergsjø, S.G., Boucher, O., Faluvegi, G., Iversen, T., Kirkevåg, A., Lamarque, J.-F., Olivié, D., Richardson, T., Shindell, D., and T. Takemura, T.: A PDRMIP Multimodel Study on the Impacts of Regional Aerosol Forcings on Global and Regional Precipitation, \*Journal of Climate\* 31, 4429-4447, doi:10.1175/JCLI-D-17-0439.1, 2018.](#)

30 Matthews, H. D., Gillet, N. P., Stott, P. A., and Zickfeld, K.: The proportionality of global warming to cumulative carbon emissions. *Nature* 459, 829–832. <https://doi.org/10.1038/nature08047>, 2009.

McJeon, H. et al.: Limited impact on decadal-scale climate change from increased use of natural gas, *Nature* 514, 482–485, 35 doi:10.1038/nature13837, 2014.

Meinshausen, M., Raper, S.C.B., and Wigley, T.M.L.: Emulating coupled atmosphere-ocean and carbon cycle models with a simpler model, MAGICC6 – Part 1: Model description and calibration. *Atmos. Chem. Phys.* 11, 1417-1456, doi:10.5194/acp-11-1417-2011, 2011a.

40 Meinshausen, M., Raper, S.C.B., and Wigley, T.M.L.: Emulating coupled atmosphere-ocean and carbon cycle models with a simpler model, MAGICC6 – Part 2: Applications. *Atmos. Chem. Phys.* 11, 1457-1471, doi:10.5194/acp-11-1457-2011, 2011b.

- Meinshausen, M. et al.: The RCP greenhouse gas concentrations and their extensions from 1765 to 2300. *Climatic Change*, 109, 213-241, 2011c.
- 5 Nicholls, R.J., Brown, S., Goodwin, P., Wahl, T., Lowe, T.J., Solan, M., Godbold, J.A., Haigh, I.D., Lincke, D., Hinkel, J., Wolff, C., and Merken, J.-L.: Stabilisation of global temperature at 1.5°C and 2.0°C: Implications for coastal areas, *Philosophical Transactions of the Royal Society A*. doi:10.1098/rsta.2016.0448, 2018.
- PANAEOSSENS project group members: Making sense of palaeoclimate sensitivity, *Nature* 491, 683-691, 2012.
- 10 Riahi, K., Rao, S., Krey, V., Cho, C., Chirkov, V., Fischer, G., Kindermann, G., Nakicenovic, N., and Rafaj, P.: RCP 8.5—A scenario of comparatively high greenhouse gas emissions, *Climatic Change*, 109,33–57, 2011.
- Smith, D. M. et al.: Earth’s energy imbalance since 1960 in observations and CMIP5 models. *Geophys. Res. Lett.* 42.4,  
15 1205–1213, 2015.
- Smith, R.S.: The FAMOUS climate model (versions XFXWM and XFHCC): description and update to version XDBUA, *Geosci. Model Dev.*, 5, 269-276, doi:10.5194/gmd-5-269-2012, 2012.
- 20 Smith, T. M., Reynolds, R. W., Peterson, T. C., and Lawrimore, J.: Improvements to NOAA’s historical merged land–ocean surface temperature analysis (1880–2006). *J. Clim.* 21, 2283–2296, 2008.
- Taylor, K. E., Stouffer, R.J., and Meehl, G.A.: An overview of CMIP5 and the experiment design, *Bulletin of the American Meteorological Society*, 93, 485-498, doi:10.1175/BAMS-D-11-00094.1, 2012.
- 25 Tebaldi, C., & Arblaster, J.M.: Pattern Scaling: Its Strengths and Limitations, and an Update on the Latest Model Simulations, *Climatic Change*, 122(3), 459–471 (2014). <http://dx.doi.org/10.1007/s10584-013-1032-9>.
- Thomson, A. M., et al.: RCP4.5: A pathway for stabilization of radiative forcing by 2100, *Climatic Change*, 109(1), 77–94,  
30 doi:10.1007/s10584-011-0151-4, 2011.
- Williams, R.G, Goodwin, P., Roussenov, V.M., and Bopp, L.: A framework to understand the transient climate response to emissions. *Environmental Research Letters*, 11, doi:10.1088/1748-9326/11/1/015003, 2016.
- 35 Williams, R.G., Roussenov, V., Goodwin, P., Resplandy, L., and Bopp, L.: Sensitivity of global warming to carbon emissions: effects of heat and carbon uptake in a suite of Earth system models, *Journal of Climate* 30, 9343-9363, doi:10.1175/JCLI-D-16-0468.1, 2017a.
- Williams, R.G., Roussenov, V., Frölicher, T.L., and Goodwin, P.: Drivers of continued surface warming after cessation of  
40 carbon emissions, *Geophysical Research Letters* 44, 10633-10642, GRL56532, doi:10.1002/2017GL075080, 2017b.
- Williamson, D., Blaker, A. T., Hampton, C., and Salter, J.: Identifying and removing structural biases in climate models with history matching. *Climate Dynamics* 45, 1299, 2015.

van Vuuren D. P. et al.: Energy, land-use and greenhouse gas emissions trajectories under a green growth paradigm, *Global Environmental Change* 42, 237–250, doi:10.1016/j.gloenvcha.2016.05.008, 2017.

5 van Vuuren, D.P. et al.: Alternative pathways to the 1.5 °C target reduce the need for negative emission technologies, *Nature Climate Change*, doi:10.1038/s41558-018-0119-8, 2018.

Vose, R. S. et al.: NOAA's merged land–ocean surface temperature analysis. *Bull. Am. Meteorol. Soc.* 93, 1677–1685, 2012.

10

Zickfeld, K., Arora, V.K., and Gillett, N.P.: Is the climate response to CO<sub>2</sub> emissions path dependent? *Geophys. Res. Lett.* 39, L05 703, 2012.

|

Reference Scenario	RCP2.6	RCP4.5	RCP8.5
RCP2.6	=	0.78	0.75
RCP4.5	2.83	=	0.17
RCP8.5	2.15	0.41	=

**Table 1: The difference between one scenario LGRTC and another, expressed as the spatially averaged number of multi-model standard deviations in LGRTC the multi-model mean LGRTC is from the second scenario relative to the first:  $\int \frac{|\mu_j - \mu_i|}{\sigma_i} dA / \int dA$ , where  $A$  is surface area,  $\mu_j$  and  $\mu_i$  are the mean LGRTC of scenarios  $j$  and  $i$ , and  $\sigma_i$  is the standard deviation in LGRTC for scenario  $i$ .**

5

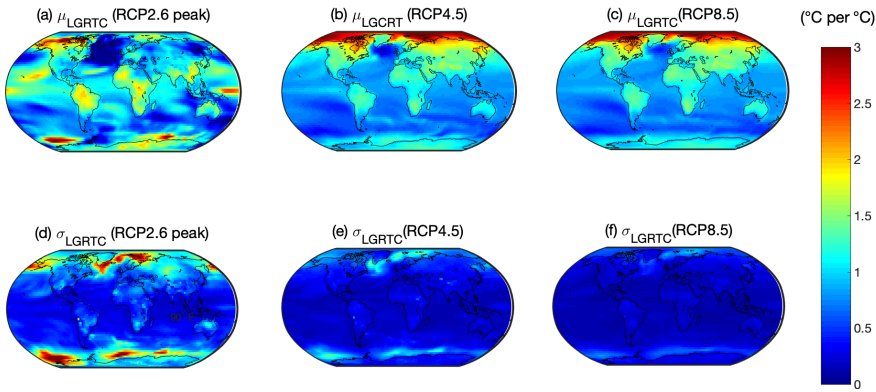


**Figure 1: The LGRTC in RCP2.6, RCP4.5 and RCP8.5 scenarios analysed from a multi-model ensemble of CMIP5 simulations. (a), (b) and (c) show the multi-model mean LGRTC,  $\mu_{LGRTC}$ , while (d), (e) and (f) show the multi-model standard deviation in LGRTC,  $\sigma_{LGRTC}$ , for each scenario.**

10

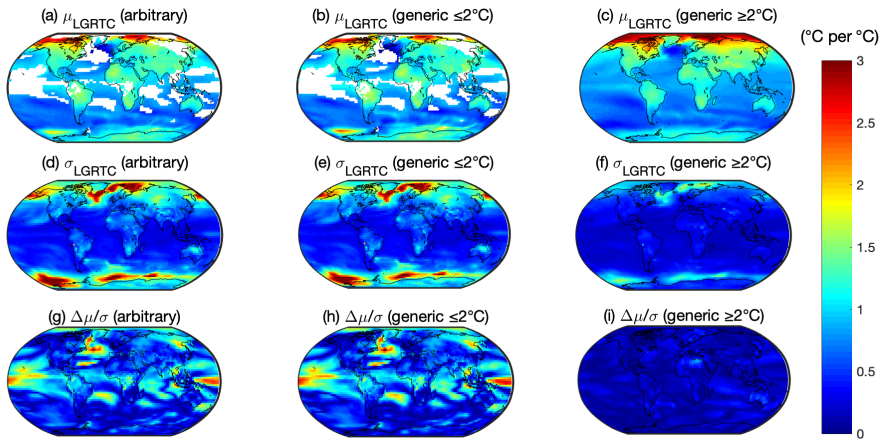


**Figure 2: The LGRTC in the arbitrary, generic  $\leq 2^\circ\text{C}$  and generic  $\geq 2^\circ\text{C}$  scenarios. Panels (a), (b) and (c) show the scenario mean LGRTC. Panels (d), (e) and (f) show the scenario standard deviation in LGRTC. Panels (g), (h) and (i) show the ratio of the maximum absolute discrepancy in the mean LGRTC from the underlying RCP scenarios,  $\Delta\mu$ , to the standard deviation in the LGRTC,  $\sigma$ , in the combined scenario:  $\Delta\mu/\sigma$ .**

5

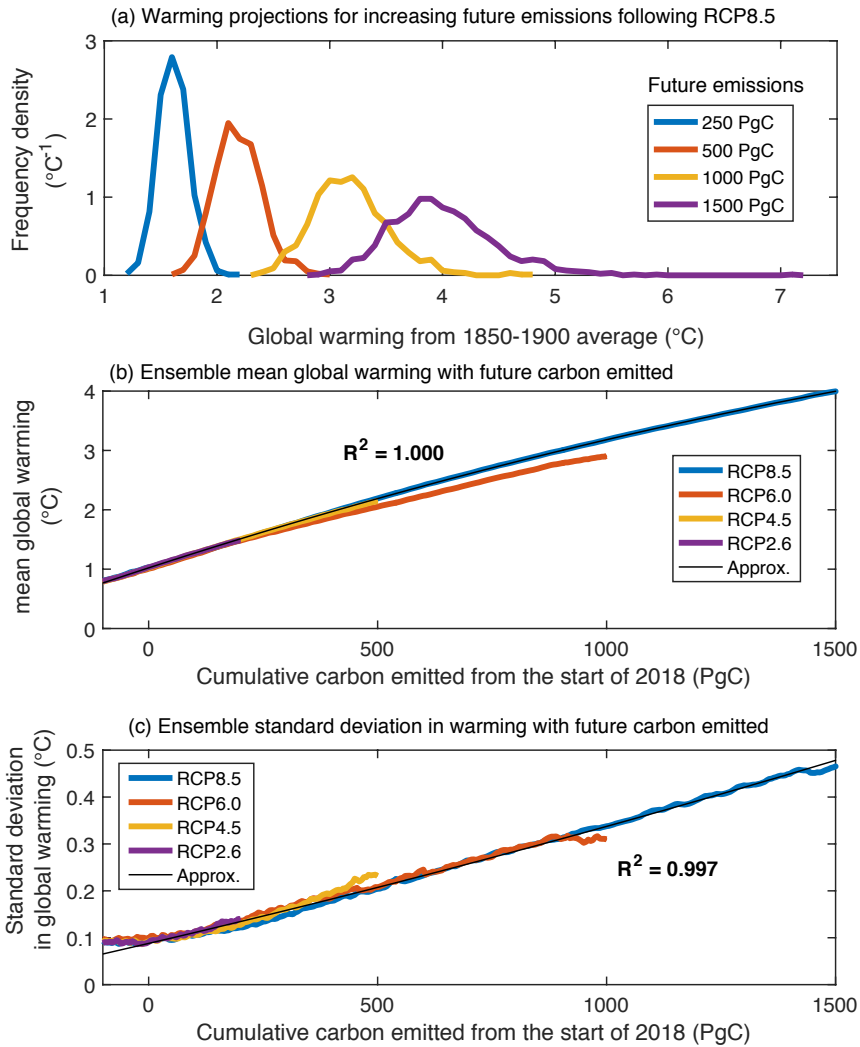


Figure 3: Projections of global mean surface warming from the history matched WASP ensemble for different future carbon emission sizes. (a) Frequency distributions of projected warming in the WASP ensemble for different future carbon emission sizes after the start of 2018. (b) Ensemble-mean global warming as future cumulative carbon emitted increases. (c) Ensemble standard deviation in global warming as future carbon emitted increases. (b) and (c) show the RCP8.5 (blue), RCP6.0 (red), RCP4.5 (orange) and RCP2.6 (purple) scenarios. A quadratic approximation, eq. 3 for (b) and eq. 4 for (c), is a good fit to the RCP8.5 scenario (thin black line). All panels show warming calculated relative to the 1850-1900 average.

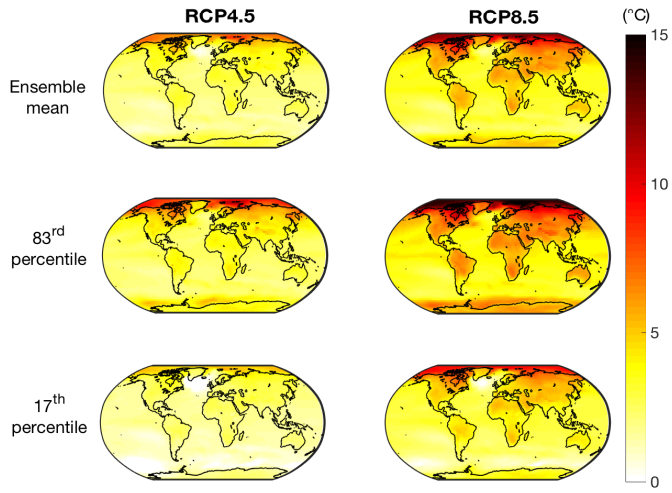


Figure 4: Projected warming for the period 2081-2100 relative to the 1850-1900 average from  $1 \times 10^3$  history matched simulations of the ultra-fast WASP/LGRTC ensemble. The left-hand column is for the RCP4.5 scenario and the right-hand column is for the RCP8.5 scenario. The top, middle and bottom rows represent the mean, 83rd percentile and 17th percentile of the model ensemble.

5

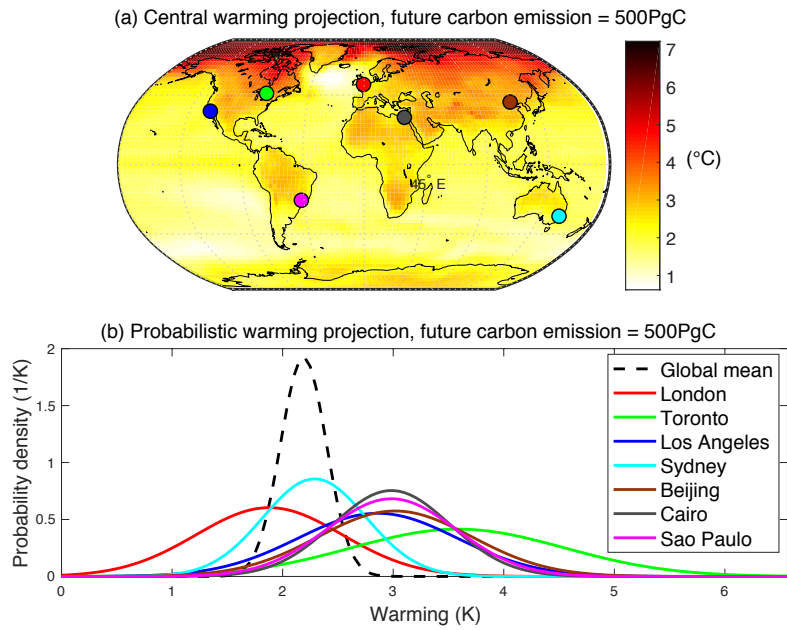


Figure 5: Warming projections when future emissions reach 500 PgC from the start of 2018. (a) The spatial distribution of the central warming projection. (b) The probability distributions of local warming for 7 locations (solid colour lines) and the global surface average (black dashed line). All warming projections given relative to the average temperature from 1850 to 1900. Global mean warming projected from the quadratic approximation to the history matched WASP ensemble (eqns. 3 to 6) using the generic >2°C spatial pattern.

Deleted: 4